



Queensland University of Technology
Brisbane Australia

This is the author's version of a work that was submitted/accepted for publication in the following source:

Shafiei, Mahnaz, Hoshyargar, Faegheh, Motta, Nunzio, & O'Mullane, Anthony P.

(2015)

Development of new gas sensors based on oxidized galinstan. In *IEEE Sensors*, IEEE, Busan Busan, South Korea, pp. 619-621.

This file was downloaded from: <http://eprints.qut.edu.au/91627/>

© Copyright 2015 IEEE

Notice: *Changes introduced as a result of publishing processes such as copy-editing and formatting may not be reflected in this document. For a definitive version of this work, please refer to the published source:*

Development of New Gas Sensors Based on Oxidized Galinstan

Mahnaz Shafiei and Nunzio Motta

Institute for Future Environments and School of Chemistry,
Physics, and Mechanical Engineering,
Queensland University of Technology (QUT)
Brisbane, QLD 4001, Australia
Email: mahnaz@ieee.org

Faegheh Hoshiyargar and Anthony P. O'Mullane

School of Chemistry, Physics, and Mechanical Engineering,
Queensland University of Technology (QUT)
Brisbane, QLD 4001, Australia
Email: anthony.omullane@qut.edu.au

Abstract— For the first time, we have fabricated and tested conductometric sensors based on oxidized liquid galinstan towards NO₂ and NH₃ gases at low operating temperatures. Galinstan based films on silicon substrates have been studied with two different loadings. Surface morphology of the films was investigated by means of field emission scanning electron microscopy (FESEM). The sensor with higher galinstan loading showed a better sensitivity, which can be attributed to a higher surface area, as confirmed by SEM. At 100°C, a detection limit as low as 1 and 20 ppm was measured for NO₂ and NH₃, respectively.

Keywords—sensor; galinstan; nitrogen dioxide; ammonia

I. INTRODUCTION

Galinstan, an alloy of 68.5% Gallium, 21.5% Indium and 10.0% Tin, is a nontoxic liquid metal which could replace mercury in thermometers thanks to its ultralow vapour pressure at room temperature [1]. However, the substitution of Mercury with this new material has been limited to very few applications such as microelectromechanical systems (MEMS) [2-3], ion sources [4] and coolants [5]. The main reason is the facile oxidation of galinstan in air. In particular at the microscale, oxidation occurs more profoundly and as a result, galinstan behaves like a gel rather than a liquid. However, this material has recently received attention for more diverse applications including a liquid metal enabled pump [6], photocatalysis [7] and as an actuator [8]. Significantly, the native semiconductor oxide, mainly gallium oxide (i.e. Ga₂O₃ [9]), on the surface of the micro droplets makes galinstan a novel material for gas sensing applications.

II. EXPERIMENTAL

5 mL acetonitrile was added to a glass vial containing 15 and 120 mg galinstan (Galinstan fluid 4N, Geratherm Medical AG, Germany) to prepare Sensor D and C, respectively; and the mixture was sonicated for 30 min. The films were prepared by drop casting the galinstan dispersion onto cleaned SiO₂/silicon substrates (7×7 mm²) at 70°C. Drop casting was repeated 10 times in order to obtain a continuous film. Two Au electrodes with a thickness of ~100 nm and separation of ~1 mm were deposited on top of the Galinstan films using an

Au coater (Leica EM-SCD005 Sputter Coater).

Structural characterization of the developed films was carried out using field emission scanning electron microscopy (FESEM, Zeiss Sigma VP field emission scanning electron microscope equipped with an Oxford XMax 50 Silicon Drift energy dispersive X-ray detector at 20 kV under high-vacuum).

The oxidized galinstan sensors were placed in a fully automated multi-channel gas testing system and tested towards NO₂ and NH₃ gases at different temperatures of 25, 50, 100 and 150°C. The system includes a 1100 mL volume test chamber capable of testing four sensors in parallel, 8 high precision mass flow controllers (MFC, MKS 1479A) to regulate the gas mixture, 8-channel MFC processing unit (MKS 647C), a picoammeter (Keithley 6487) and a climatic chamber to control the temperature as shown in Fig. 1. The sensors were heated at the desired temperature using a micro-ceramic heater. Certified gas cylinders of high purity (99.999%) dry synthetic air and low concentrations of analyte gases, 12.2 ppm NO₂ and 99 ppm NH₃ balanced in synthetic air were used. The desired concentration of the target gas was obtained by adjusting the respective flow rates via the MFCs, while maintaining a total constant flow rate of 200 sccm (mL/min). The response upon exposure to the target gas was evaluated by measuring a change in the sensors resistance while a bias voltage of 1 V was applied.

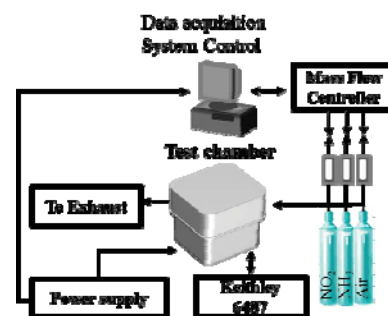


Fig. 1. Schematic representation of the gas sensing set-up.

III. RESULTS AND DISCUSSION

SEM images (Fig. 2) revealed micro-scale droplets with different dimensions. Better coverage on the substrate was observed for Sensor C when compared to Sensor D. A film thickness of 10-12 μm was measured for Sensor C (Fig.2c).

The electrical and gas sensing performance of the devices were investigated towards NO_2 and NH_3 at 25, 50, 100 and 150 $^\circ\text{C}$. The sensors did not show any response to NH_3 at temperatures below 100 $^\circ\text{C}$ while there was an appreciable response to NO_2 , however the sensors did not fully recover and the baseline drifted. The highest response with a more stable baseline was measured at 100 $^\circ\text{C}$ for both gases.

The sensors exhibited a decrease in their resistivity upon exposure to oxidizing NO_2 gas, i.e. galinstan film showed p-type behavior (Fig. 3). A higher response was recorded for Sensor C than Sensor D (Table I), probably due to better film coverage as confirmed by SEM and therefore higher active surface area for gas interaction. For Sensors C and D, a 7.7% and 5.37% response was recorded respectively.

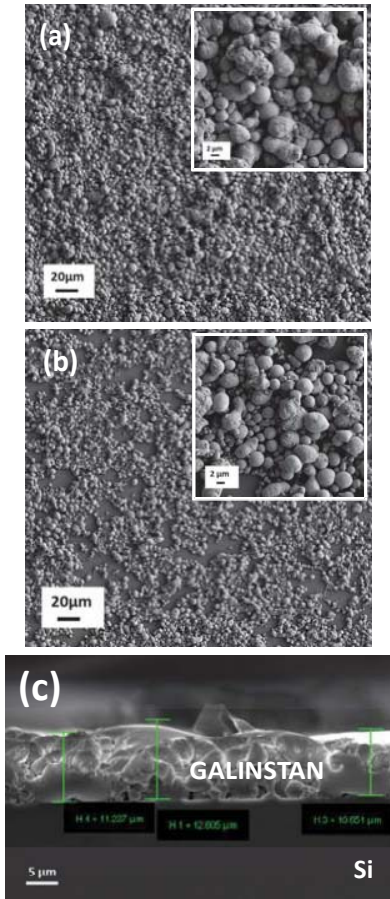


Fig. 2. SEM images of as-deposited galinstan films in (a) Sensor C, (b) Sensor D. (c) film thickness in Sensor C (10-12 μm).

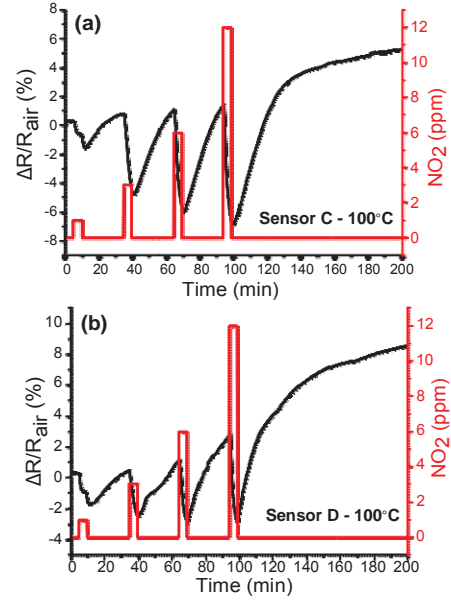


Fig. 3. Dynamic response of (a) Sensor C and (b) Sensor D towards NO_2 gas at 100 $^\circ\text{C}$.

The response (R) was calculated according to:

$$R(\%) = 100 \times ((R_{\text{air}} - R_{\text{gas}})/R_{\text{air}}) \quad (1)$$

where R_{air} is the film resistance under synthetic air and R_{gas} is the film resistance upon exposure to the target gas.

As shown in Fig. 4, p-type behaviour was observed towards the reducing gas, NH_3 . As expected, NH_3 acts as an electron donor thus leading to an increase in the resistivity of the galinstan film that exhibits p type behaviour. A response of 1.16% and 0.798% was measured for Sensors C and D, respectively (Table II).

After testing the sensors up to 150 $^\circ\text{C}$, they were tested again at 25 $^\circ\text{C}$ to investigate the effect of such low temperature annealing on the electrical properties of the films and thus their sensing performance. A significant improvement in the response was observed, however the sensors still did not recover to the original baseline. It is noteworthy that the sensors showed a response to NH_3 gas at 25 $^\circ\text{C}$ while the as-deposited sensors did not show any response below 100 $^\circ\text{C}$. The resistivity of Sensors C and D increased from 9.8 and 15.5 kn to 82 and 60 kn, respectively, by presumably more pronounced oxidation of surface metals.

TABLE I. RESPONSE (%) OF THE SENSORS TOWARDS NO_2 AT OPTIMAL OPERATING TEMPERATURE OF 100 $^\circ\text{C}$

Sensor	NO_2 (ppm)			
	1	3	6	12
C	1.72	5.41	6.88	7.7
D	1.91	2.97	3.88	5.37

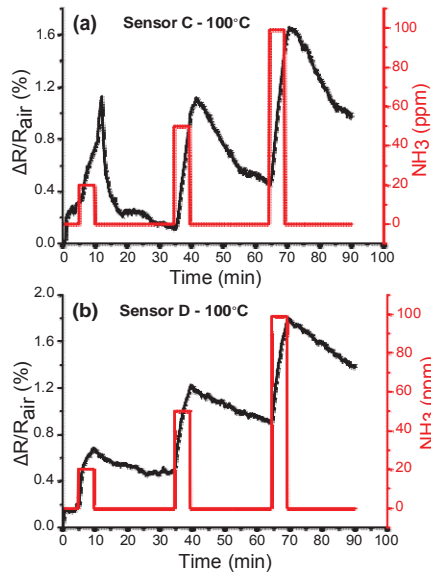


Fig. 4. Dynamic response of (a) Sensor C and (b) Sensor D towards NH_3 gas at 100°C

TABLE II. RESPONSE (%) OF THE SENSORS TOWARDS NH_3 AT OPTIMAL OPERATING TEMPERATURE OF 100°C

Sensor	NH_3 (ppm)		
	20	50	99
C	0.85	0.95	1.16
D	0.5	0.68	0.798

The sensors were subsequently tested up to 200°C . An improvement in recovery was observed but the response of the samples degraded significantly after prolonged heat treatment. SEM investigation revealed that the droplets were locally collapsed (Fig. 5) resulting in a reduction of the surface area and hence gas interaction.

IV. CONCLUSION

In this paper, the NO_2 and NH_3 gas sensing performance of oxidized galinstan films with two different loadings was investigated. The SEM analysis revealed micro-scale droplets with better coverage for the film with higher loading. The developed sensors showed the highest response with a more stable baseline at 100°C with a detection limit as low as 1 and 20 ppm for NO_2 and NH_3 , respectively. The sensor with the higher loading of galinstan showed a higher response due to better film coverage. Further experiments are needed in order to improve the response and recovery time. The experimental results demonstrated that oxidized galinstan is a promising material for gas sensing applications at low temperatures.

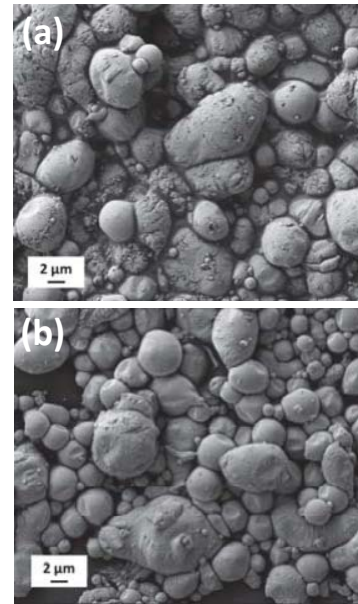


Fig. 5. SEM images of galinstan films in (a) Sensor C and (b) Sensor D after the testing up to 200°C .

ACKNOWLEDGMENT

The data reported in this paper were obtained at the *Central Analytical Research Facility* operated by the *Institute for Future Environments* (QUT). Access to CARF is supported by generous funding from the Science and Engineering Faculty (QUT).

REFERENCES

- [1] Geratherm Medical AG, Galinstan Safety Data Sheet, Jul. 20, 2011. [Online]. Available: <http://www.rgmd.com/msds/msds.pdf>
- [2] A. Cao, P. Yuen, and L. Lin, "Microrelays with bidirectional electrothermal electromagnetic actuators and liquid metal wetted contacts," *J. Microelectromech. Syst.*, vol. 16, no. 13, pp. 700–708, 2007.
- [3] P. Sen and C.-J. Kim, "A fast liquid-metal droplet microswitch using EWOD-driven contact-line sliding," *J. Microelectromech. Syst.*, vol. 18, no. 1, pp. 174–185, 2009.
- [4] R. Clampitt and D. K. Jefferies, "Miniature ion sources for analytical instruments," *Nucl. Instrum. Methods*, vol. 149, no. 1–3, pp. 739–742, 1978.
- [5] A. H. Fleitman and J. R. Weeks, "Mercury as a nuclear coolant," *Nucl. Eng. Des.*, vol. 16, pp. 266–278, 1971.
- [6] S.-Y. Tang, K. Khoshmanesh, V. Sivan, Ph. Petersen, A. P. O'Mullane, D. Abbott, A. Mitchell, and K. Kalantar-zadeh, "Liquid metal enabled pump," *PNAS*, vol. 111, pp. 3304–3309, 2014.
- [7] W. Zhang, J. Zhen Ou, S.-Y. Tang, V. Sivan, D. D. Yao, K. Latham, K. Khoshmanesh, A. Mitchell, A. P. O'Mullane, and K. Kalantar-zadeh, "Liquid metal/metal oxide frameworks," *Adv. Funct. Mater.*, vol. 24, pp. 3799–3807, 2014.
- [8] S.-Y. Tang, V. Sivan, K. Khoshmanesh, A. P. O'Mullane, X. Tang, B. Gol, N. Eshtiaghi, F. Lieder, Ph. Petersen, A. Mitchell, and K. Kalantar-zadeh, "Electrochemically induced actuation of liquid metal marbles," *Nanoscale*, vol. 5, pp. 5949–5957, 2013.
- [9] F. Scharmann, G. Cherkashinin, V. Breternitz, Ch. Knedlik, G. Hartung, Th. Weber and J. A. Schaefer, "Viscosity effect on GaInSn studied by XPS," *Surf. Interface, Anal.*, vol. 36, pp. 981–985, 2004.